


# Low energy consumption spintronics using multiferroic heterostructures

**Review Article****Author(s):**

Trassin, Morgan 

**Publication date:**

2016-01

**Permanent link:**

<https://doi.org/10.3929/ethz-b-000108606>

**Rights / license:**

[Creative Commons Attribution-NonCommercial-NoDerivatives 4.0 International](#)

**Originally published in:**

Journal of Physics: Condensed Matter 28(3), <https://doi.org/10.1088/0953-8984/28/3/033001>

**Funding acknowledgement:**

144988 - Structured oxides with magnetoelectric and charge-transport functionalities (SNF)

Topical Review

# Low energy consumption spintronics using multiferroic heterostructures

Morgan Trassin

Department of Materials, ETH Zurich, Vladimir-Prelog-Weg 4, 8093 Zurich

E-mail: [morgan.trassin@mat.ethz.ch](mailto:morgan.trassin@mat.ethz.ch)

## Abstract

We review the recent progress in the field of multiferroic magnetoelectric heterostructures. The lack of single phase multiferroic candidates exhibiting simultaneously strong and coupled magnetic and ferroelectric orders led to an increased effort into the development of artificial multiferroic heterostructures in which these orders are combined by assembling different materials. The magnetoelectric coupling emerging from the created interface between the ferroelectric and ferromagnetic layers can result in electrically tunable magnetic transition temperature, magnetic anisotropy or magnetization reversal. The full potential of low energy consumption magnetic based devices for spintronics lies in our understanding of the magnetoelectric coupling at the scale of the ferroic domains. Although the thin film synthesis progresses resulted into the complete control of ferroic domain ordering using epitaxial strain, the local observation of magnetoelectric coupling remains challenging. The ability to imprint ferroelectric domains into ferromagnets and to manipulate those solely using electric fields suggests new technological advances for spintronics such as magnetoelectric memories or memristors.

Keywords: multiferroics, BiFeO<sub>3</sub>, magnetoelectrics, artificial multiferroics, spintronics, ferroic domain imprint, multiferroic memristor.

## **1. Introduction**

*1.1 Magnetoelectric multiferroic heterostructures*

*1.2 Low energy consumption spintronics and multiferroics*

## **2. Acting on magnetism using voltage in multiferroic heterostructures**

*2.1 Electric field control of magnetic anisotropy*

*2.2 Controlling magnetic ordering temperature*

*2.3 Electric field modulation of exchange bias*

*2.4 Room temperature electric field induced magnetization reversal*

## **3. The role of ferroic domains and domain imprint**

*3.1 Ferroelectric domain engineering*

*3.2 Strain induced polarity*

*3.3 Ferroelectric domain imprint in multiferroic heterostructures*

## **4. Multiferroic heterostructures for spintronics**

*4.1 Magnetoelectric multiferroic memories*

*4.2 Multiferroics in magnetic nanologics*

*4.3 Multiferroic memristors*

## **5. Future perspectives and concluding remarks**

*5.1 Towards single domain switching*

*5.2 Magnetoelectric switching dynamics*

## **Acknowledgements**

## **References**

## 1 Introduction

### 1.1 Magnetoelectric multiferroic heterostructures

Materials possessing two or more ferroic orders, such as ferromagnetism, ferroelasticity or ferroelectricity, in a single phase are defined as multiferroics [1]. For application purposes, materials possessing coexisting ferroelectricity and ferromagnetism are mainly targeted. Symmetry considerations, orbital configurations and chemistry related arguments explain the rareness of multiferroic materials possessing a non-zero electric polarization coexisting with a net magnetization [2]. Most of the existing multiferroic materials are ferroelectric and anti-ferromagnetic, i. e. exhibiting an electrically switchable ferroelectric polarization but no net magnetization. Two types of multiferroic classes can be defined, the proper and the improper multiferroics [3]. This classification refers to the origin of the ferroelectric order parameter. In proper multiferroics the ferroelectricity emerges via the classical stabilization of off-centered ions leading to a macroscopic electric dipole [4]. Most of these compounds crystallize into the perovskite structure [5,6]. Improper multiferroics present a ferroelectric order originating from another symmetry breaking [7] or from a magnetic frustration leading to an atomic displacement due to inverse Dzyaloshinskii Moriya interaction [3,8,9]. Within the multiferroic materials, the so-called magnetoelectric multiferroic materials [10,11] exhibit a coupling between the above mentioned ferroic orders, leading to possible electrically induced modification of the magnetic state or the change of ferroelectric properties under a magnetic field. Despite the considerable research efforts in the field, only a few single phase materials present established multiferroic magnetoelectric properties at room temperature [6,12,13,14]. The most studied room temperature multiferroic is  $\text{BiFeO}_3$ , this material possesses a strong ferroelectric polarization coupled to an antiferromagnetic ordering [15,16]. In thin film form, depending on the strain state, the magnetic cycloid present in the bulk form can be broken [17], leading a coexisting ferroelectric order and weak ferromagnetism behavior [6,18].

To overcome the lack of candidates for room temperature multifunctional applications, increasing efforts were put into multiferroic heterostructures, also called artificial multiferroics [19,20]. In these multilayered systems, multiferroic and magnetoelectric behavior are induced via interfacing ferromagnetic and ferroelectric thin films. The correlation between piezoelectricity, magnetoelasticity and magnetoelectricity established for single phase materials [1] can be rearranged when combining ferroic properties in heterostructures as shown in the Figure 1.

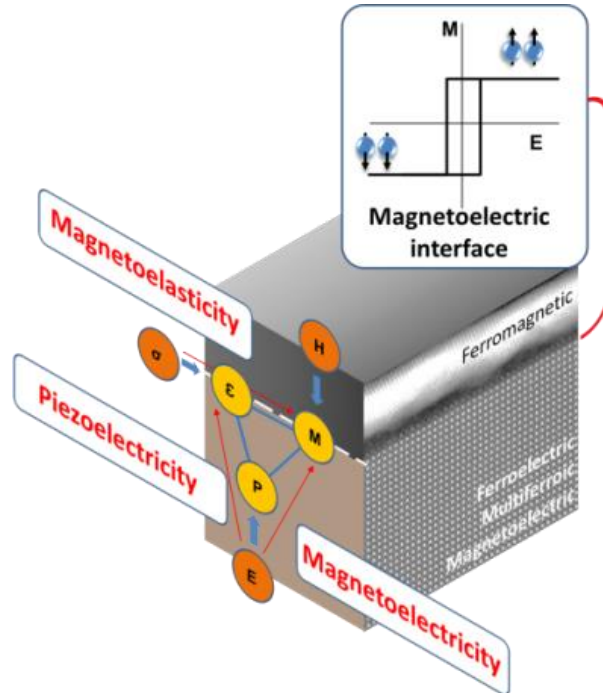


Figure 1. Multiferroic heterostructure. The electric field  $E$ , magnetic field  $H$ , and stress  $\sigma$  control the electric polarization  $P$ , magnetization  $M$ , and strain  $\epsilon$ . When a ferroelectric or magnetoelectric multiferroic material is combined with a ferromagnet, a magnetoelectric interface can be achieved via the cross coupling between piezoelectricity, magnetoelasticity and magnetoelasticity.

The full set of functionalities of the multiferroic heterostructure resides at the created interface, where charge [21], strain [22,23] and interface induced magnetization [24] can play a major role in the macroscopic magnetoelectric coupling. The use of a ferroelectric or magnetoelectric multiferroic compound allows for electrical control of interfacial strain ( $\epsilon$ ), polarization ( $P$ ) or charge state, weak ferromagnetism order ( $M$ ) or antiferromagnetic order via the piezoelectricity, ferroelectric polarization and magnetoelastic coupling, respectively. The ferromagnetic layer grown on top, enables then, the propagation of the interfacial states into a material with a net moment via magnetostriction, exchange coupling or exchange bias [19]. In such ferroelectric/ferromagnetic heterostructures, the achievement of electrically controllable net magnetization (see Figure 1) becomes conceivable.

### 1.2 Low energy consumption spintronics and multiferroics

Following the discovery of the giant magnetoresistance [25,26], the awareness of the use of the electron spin as a new degree of freedom for electronics led to the emergence of the spintronics research field. In the so-called spin valves devices, described in the Figure 2, the electron scattering or tunneling between

two ferromagnetic layers (layer I and II in Figure 2) is selectively activated by controlling the spin orientation. The efforts of the scientific community focused first in the optimization of the devices and the enhancement of the resistance difference between the low and high resistance states, i. e. parallel and anti-parallel configurations of the ferromagnetic electrodes (see Figure 2). The interest evolved then towards energy efficient spintronics devices and the search for the energy minimization of the ferromagnetic moment reversal. To control the spin state, the energy-consuming external magnetic field was replaced by spin polarized current injection [27,28]. In the spin transfer torque (STT) based devices, a flow of polarized electrons is used to set the low or high resistance state. Based on the spin torque transfer, high spin polarized current density can indeed reverse a magnetization state. The use of the transmitted or reflected flow allows the achievement of two magnetoresistance states [29] as sketched in the Figure 2. Manipulation of magnetization by current is not limited to STT and it is now well established that the conversion of a charge current into a spin current driven by spin-orbit interaction such as the spin Hall effect (SHE) [30] and Rashba-Edelstein effect [31] in non-magnetic material leads to strong spin-orbit torques (SOT) [32]. The use of these SOTs allowed experimental observations of perpendicular and in-plane magnetization reversals in Pt/Co, Ta/CoFeB and W/CoFeB based heterostructures [33,34,35]. The switching mechanism is involving the SHE generated in the heavy metal layer, i. e. the SHE deflects electrons relatively to their spin orientation, giving rise to pure spin currents transverse to an applied charge current [36] (Figure 2). All these advances led to the development of new memories, the most advanced one being proposed by Parkin and coworkers with the race track memory concept [37]. The information is contained in a ferromagnetic domain wall and manipulated using spin currents.

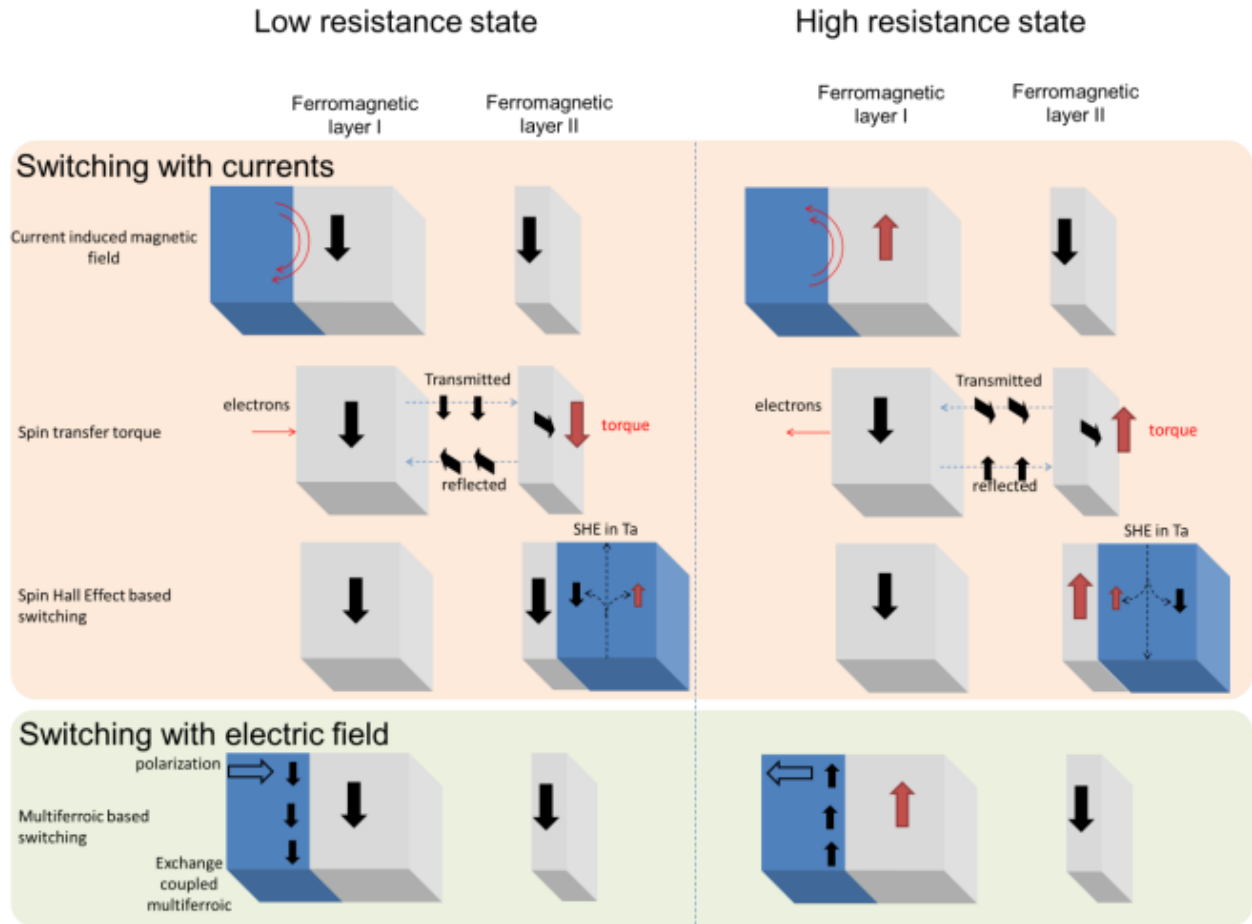


Figure 2. Switching a ferromagnetic state in a spin valve architecture. Using electrical currents, a magnetic state can be altered by the emerging current induced magnetic field, the spin transfer torque or spin orbit torque. When the multiferroic magnetoelectric materials are considered a voltage is sufficient to reverse the ferromagnet layer.

Nevertheless, the use of current results in energy dissipation via Joule effect, therefore ways to control a magnetic state simply by applying a voltage are constantly investigated. In this field several achievement have been accomplished with the use of ultra-fast voltage pulses [38] or with magnetostrictive devices [39] but an external magnetic field bias is required to break the time reversal symmetry breaking necessary to reverse a magnet. Therefore multiferroic magnetoelectrics in which both inversion and time reversal symmetry are broken [19] are considered to play a major role in the future of low energy consuming spintronics. The insertion of magnetoelectrics multiferroics is sketched in the Figure 2. An electric field is used to reverse the magnetic order in the magnetoelectric multiferroic compound via the magnetoelectric coupling, and the ferromagnetic layer moment is reversed via interfacial coupling.

## 2 Acting on magnetism using voltage in multiferroic heterostructures

As mentioned in the introduction section, multiferroic heterostructures present high potential for low energy consumption spintronics devices. In this section, the progresses regarding electrically induced modification of magnetic response in thin film heterostructures will be reviewed.

### 2.1 Electric field control of magnetic anisotropy in metal oxide heterostructure.

*Magnetostriction:* Among the possible pathways towards electrical modification of magnetic anisotropies in multiferroic heterostructures, the most investigated route involves the combination of piezoelectricity and magnetostriction. Due to the hysteretic nature of the ferroelectric materials response to an external electric field, non-volatile and reversible effect can be expected [40]. Van Dijken and coworkers [22,41,42] have been focusing their efforts in the observation of the effect of ferroelectric BaTiO<sub>3</sub> substrate strain transfer into a crystalline CoFe ferromagnetic layer. Using magneto optic Kerr effect imaging (MOKE), they were able to visualize the substrate imprint into the ferromagnetic layer. The elastic coupling between magnetic and ferroelectric domain results in the transfer of the substrate domain pattern into the ferromagnetic domain structure. Furthermore, the application of a voltage, inducing ferroelectric ferroelastic switching events in the BaTiO<sub>3</sub> substrate, caused ferromagnetic domains movements and 90° magnetic easy axis rotations [22,43]. For an efficient electrically induced effect, high magnetostrictive coefficient ferromagnets are favored [44,45] and the ferroelectric ferroelastic switching event has to drive a noticeable strain variation. For instance, in a purely c-oriented tetragonal ferroelectric system such as BaTiO<sub>3</sub>, 180° switching results in identical initial and final strain states. In order to create strain variation, switching events involving in-plane component of the ferroelectric polarization have to be electrically stimulated [22]. Mixed in-plane and out-of-plane oriented domain states, i. e. a- and c- domains, structured BaTiO<sub>3</sub> and Pb(Zr<sub>0.2</sub>Ti<sub>0.8</sub>)O<sub>3</sub> (PZT), (1-x)[Pb(Mg<sub>1/3</sub>Nb<sub>2/3</sub>)O<sub>3</sub>]-x[PbTiO<sub>3</sub>] (PMNPT) are usually combined with high Curie temperature ferromagnets such as NiFe [46], CoFe [22,42,43,47] or Ni [48,49,50,51,52]. These effects are not restricted to electrically induced in-plane magnetic axes rotations; in-plane to out-of-plane magnetic axis rotations have also been observed using high magnetostrictive coefficient [45] materials such as Tb<sub>0.3</sub>Dy<sub>0.7</sub>Fe<sub>2</sub> (Terfenol-D) [53,54]. The magnetostrictive approach is also under intense investigation in full oxide heterostructures [55,56]. In the oxide heterostructure BiFeO<sub>3</sub>/PMNPT sketched in the figure 3a, the application of a voltage results in PMNPT crystal substrate lattice parameter reversible variations, as shown in Figure 3b. The corresponding variation on epitaxially grown BiFeO<sub>3</sub> lattice parameter is shown in Figure 3c. Such a capacity opens the way towards reversible lattice parameter changes and therefore tunable strain states and magnetostriction effect strength. In epitaxial heterostructures however,



additional degrees of freedom such as orbital ordering at epitaxial interfaces lead to more complex phenomena and challenging understanding [57].

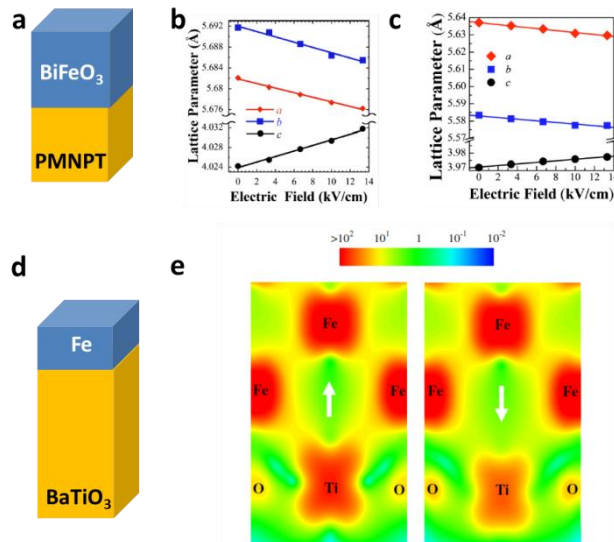


Figure 3. a-c) Strain in oxide heterostructures and surface magnetoelectric effect. The effect of applied voltage in the BiFeO<sub>3</sub>/PMNPT heterostructure sketched in a) results in reversible non-negligible substrate and film lattice parameter changes in b) and c), respectively. Reprinted with permission from [56].

Copyright 2010, AIP Publishing LLC. In the Fe/BaTiO<sub>3</sub> heterostructure sketched in d), the ferroelectric polarization (white arrow) affects the spin charge distribution at the interface between the ferromagnetic metal and the ferroelectric BaTiO<sub>3</sub> crystal in e). Reprinted figure with permission from [60]. Copyright 2006 by the American Physical Society.

However, strain being uniaxial rather than unidirectional, no deterministic magnetization 180° reversal can be expected and the application of voltage to such heterostructures is therefore restricted to 90° magnetic axis rotations. To overcome this non directional issue, Wang and coworkers considered the influence of magnetic shape anisotropy [58]. Their mesoscale phase field simulation approach, considering patterned single domain magnets on ferroelectric substrates, highlighted the possibility to induce a two-step magnetization rotation mechanism by an external electric field. The two 90° rotations sum up to a final full reversal of the magnetization of the ferromagnetic dots. This paves the way to potential ultra-low energy consuming and high efficiencies in magnetoresistance based spintronics devices.

*Surface magnetoelectric effect:* As an alternative to strain acting on a magnet, Tsymbal and coworkers investigated using density-functional calculations, the influence of external electric field on surface

magnetization and surface magnetocrystalline anisotropy of thin ferromagnetic layers [59,60,61,62]. In a ferromagnetic metallic layer, the conduction electrons will screen any external electric field over the corresponding screening length. The ferromagnetic nature of the metal will lead to spin dependent screening [63]. When considering a dielectric/metal heterostructure, the effect of the electric field on the ferromagnetic order is however limited to the metal surface and results in non-negligible linear changes in the surface magnetization and the surface magnetocrystalline anisotropy of a ferromagnetic metal. This effect is enhanced when replacing the so far considered dielectric component from which the interfacial charges will be induced, by a ferroelectric system as in the case of the BaTiO<sub>3</sub>/Fe heterostructure [60]. In the Figure 3 d and e, the predicted influence of the ferroelectric polarization on the charge density at the ferromagnetic/ferroelectric interface is shown. The overlap between the Ti and Fe electronic clouds is much stronger for one particular ferroelectric polarization direction (upwards in the Figure 3e), therefore a drastic change in the Fe magnetic behavior can be expected as a function of an applied voltage. These predictions have been experimentally confirmed with the observation of voltage induced magnetic anisotropy changes in magnetic tunnel junctions [64,65,66] and lead to the observation of an electric field assisted spin valve switching [67]. The reversible and coherent ferromagnetic layer magnetization reversal using voltage pulses was finally observed in 2012 under a static external magnetic field bias [38].

Surprisingly, in some systems, the electric field influence on the ferromagnetic state can expand over several unit cells within the ferromagnetic layers [68,69]. Berakdar and coworkers [70] developed a theory based on the formation of a non collinear interfacial spiral spin texture emerging from the interface. The expansion of the ferromagnetic volume influence by the external electric field is then attributed by the large spin-diffusion length in the ferromagnetic metals.

## *2.2 Controlling magnetic ordering temperature*

So far, the influence of the external electric field on the magnetic anisotropy has been described. An electric field in some cases can also disturb the origin of the magnetic order itself. For instance, in the case of the low temperature semiconductor (In,Mn)As [71,72] or (Ga,Mn)As [73]. In this particular class of materials, ferromagnetism is governed by the holes concentrations which provide the interaction between local Mn moments [74]. An electric field modulates the holes concentration and therefore the strength of the magnetic interaction within the semiconductor. A change of up to 20 K in the Curie temperature has been observed solely using an electric field [72]. This voltage modulation also results in electrically adjustable magnetic coercivity, as shown in the Figure 4 a. The effect of electric field on ordering temperature is rarely considered in room temperature multiferroic heterostructures. The most

prominent example was reported in the  $\text{PbZr}_{0.2}\text{Ti}_{0.8}\text{O}_3/\text{La}_{0.8}\text{Sr}_{0.2}\text{MnO}_3$  (PZT/LSMO) heterostructure. Here Molegraaf and coworkers [75] reported the magnetic moment and critical temperature modulation with charge concentration. By applying an electric field, the polarization of the ferroelectric layer was reversed, changing the polar state at the interface ferroelectric/colossal magnetoresistance [76] (CMR) manganite. The magnetic ordering being dependent on the charge in the CMR compound, a Curie temperature variation of up to 20 K was observed in these heterostructures. The effect opened new perspectives into manganite based multilayers since a modulation of the magnetic moment can be achieved electrically, see Figure 4 b, and led to several exciting observations in similar LSMO/ferroelectric layer interfaces [77,78]. Recently, x-ray absorption measurements showed the electric field influence on the manganite's orbital occupation in a LSMO/PZT heterostructure [79]. Likewise, the electrical modulation of the competition between ferromagnetic and antiferromagnetic instability through the magnetoelectric coupling in  $\text{BiFeO}_3/\text{La}_{0.5}\text{Ca}_{0.5}\text{MnO}_3$  (BFO/LCMO) has been shown [80]. More recently the focus shifted towards acting on the first order transition temperature in FeRh alloys [81] using magnetostrictive heterostructures [82,83]. This particular compound exhibits indeed a transition from antiferromagnetic to ferromagnetic state at around 350 K [83]. Several concepts based on ferroelectric/FeRh heterostructures were developed in order to electrically go from the antiferromagnetic to ferromagnetic phase at a fixed temperature. The experimental observation was realized by Cherifi and coworkers [83], see Figure 4 c. A shift of 25 K of the transition temperature was measured. This modulation of the magnetic moment, at a fixed temperature, is performed by applying only a few volts to the ferroelectric/FeRh heterostructure.

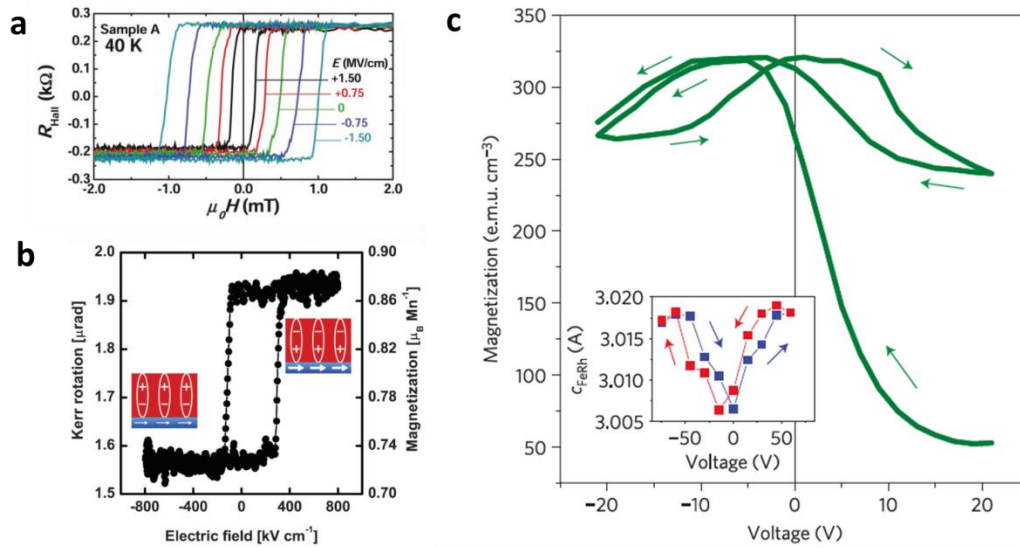


Figure 4. Controlling ferromagnetic ordering with electric field. a) Electric field modulation of magnetic coercivity in  $(In,Mn)As$  ferromagnetic semiconductor. From [72] Reprinted with permission from AAAS. b) Magnetization of LSMO layer as a function of the applied electric field in LSMO/PZT heterostructure. From [75] reproduced with permission (copyright 2009 Wiley-VCH Verlag GmbH & Co. KGaA). c) Voltage dependence of the magnetization of a FeRh layer grown on top of a  $BaTiO_3$  crystal, the FeRh lattice parameter changes are shown in inset. Reprinted by permission from Macmillan Publishers Ltd: Nature Materials from [83]. Copyright 2014.

Using the same system Marti and coworkers [84] are developing a new type of device using antiferromagnet for spintronics, and presented the FeRh based antiferromagnet memory resistor (so-called memristor).

### 2.3 Electric field modulation of exchange bias

Most of the ferroelectric multiferroics are antiferromagnetic due to orbital filling considerations [2], the main goal of their insertion into devices was therefore first directed to the electrical modification of the antiferromagnetic ordering towards voltage induced exchange bias shifting in multiferroic/ferromagnet heterostructure [19]. When coupling a ferromagnetic layer to an antiferromagnetic compound, the pinning of the antiferromagnetic state at the magnetic interface results in asymmetric ferromagnetic hysteresis loops when sweeping the external magnetic field. One of the pioneering works dealing with the insertion of multiferroic material thin films in order to electrically control the exchange bias between the ferroelectric-antiferromagnetic state and an adjacent ferromagnetic layer is employing the

hexagonal manganite  $\text{YMnO}_3$  thin film capped with 15 nm thick NiFe permalloy layer [85]. The  $\text{YMnO}_3$  system is established to be an improper multiferroic with a high ferroelectric ordering temperature (900 K) and antiferromagnetic order below 90 K [85,86]. The antiferromagnetic nature of the  $\text{YMnO}_3$  resulted in the exchange bias coupling and therefore a shift of the permalloy magnetic hysteresis towards negative field at low temperature as shown in the Figure 5 a. The application of an electric field led to the disappearance of this shift, see Figure 5 a and 5 b. Here, the mechanism is based on the pinning of magnetic domain motion at the magnetoelectric multiferroic domain walls [86]. After application of an electric field these pinning sites are moved or annihilated, resulting in a decrease of coercivity for the permalloy. These results showed the potential of multiferroic thin films and revealed the impact of multiferroics for efficient electrical control on magnetic coupling based devices.

Later, the room temperature multiferroic magnetoelectric  $\text{BiFeO}_3$  was inserted into a spin valve structure ( $\text{BiFeO}_3/\text{CoFe}/\text{Cu}/\text{CoFe}$ ) and the exchange bias coupling was evidenced at room temperature [87], the effect of electric field to the structure was then discussed. The electrical modulation of giant magnetoresistance in  $\text{BiFeO}_3$  based spin valve heterostructure was performed in 2013 [88], see Figure 5 c. Here again irreversible changes in the multiferroic layer domain configuration resulted in modified interfacial magnetic coupling and therefore in exchange bias amplitude changes. Once again the interfacial coupling mechanism involves the multiferroic domain state [89]. It is established that  $\text{BiFeO}_3$  can exhibit three types of ferroelectric domain walls making  $71^\circ$ ,  $109^\circ$  and  $180^\circ$  polarization angle at the domain walls. Martin and coworkers [90] revealed that  $109^\circ$  domain wall play a critical role in exchange bias type heterostructures and the presence of uncompensated spins at these walls is suggested [90,91]. These walls are however not stable under the application of an electrical field due to their high elastic strain state [88,92]. The reversible electrical control of exchange bias was finally achieved in a full oxide heterostructure  $\text{BiFeO}_3/\text{LSMO}$  bilayer below the blocking temperature of 100 K [93].

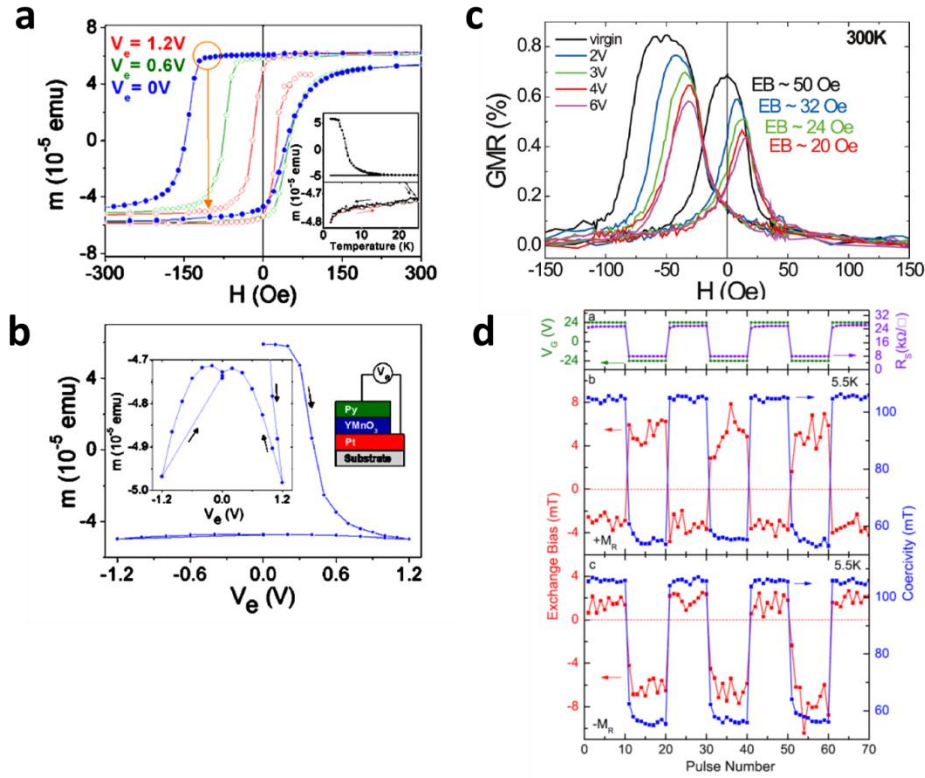


Figure 5. Electric field modulation of exchange bias. a) The exchange bias can be electrically annihilated in the  $\text{YMnO}_3/\text{NiFe}$  heterostructure. b) Under an external magnetic field, this corresponds to a reversal of magnetization. Reprinted figure with permission from [85] Copyright 2006 by the American Physical Society. c) Electric field induced reduction of exchange bias coupling in  $\text{BiFeO}_3$  based spin valve. Reprinted with permission from [88] Copyright 2012 American Chemical Society. d) Bipolar reversible control of exchange bias in  $\text{BiFeO}_3/\text{LSMO}$  heterostructure. Reprinted figure with permission from [95] Copyright 2013 by the American Physical Society.

The demonstration was first achieved using a single voltage polarity [94] and the bipolar modulation followed after optimization of the device orientation [95], see figure 5 d. Among the recent studies dealing with electrical control of magnetization in multiferroic heterostructures the  $\text{BiFeO}_3$  based bilayers showed the most promising results. The investigation of the strength of the magnetic coupling between the multiferroic layer and the ferromagnet LSMO or CoFe were carried out in order to establish the critical thickness involved [96,97]. It has been shown that although the ferroelectric state in  $\text{BiFeO}_3$  thin films is rather robust down to 4-5 unit cells [98], the antiferromagnetic state necessary to induce the exchange bias coupling is only present for thicknesses above 6 to 7 unit cells [96,97].

## *2. 4 Room temperature electric field induced magnetization reversal*

One of the main motivations to pursue the investigation in multiferroic heterostructures for spintronics was to achieve electrically a magnetic state reversal. This requires the ability to alter time reversal symmetry which is not possible by means of an electric field. In ferroelectric/ferromagnetic multiferroic heterostructures both symmetries are broken [19]. In addition, in order to efficiently act on the magnetic order parameter with an applied voltage, the multiferroic heterostructure has to exhibit magnetoelectric coupling [10]. The achievement of electrically induced magnetization reversal at room temperature was first observed in BiFeO<sub>3</sub> (in which, both inversion symmetry and time-reversal symmetry are broken) based heterostructures [99,100].

The high potential of multiferroic magnetoelectric heterostructure was first highlighted in 2006 by Zhao and coworkers [101]. In this work, a change in the antiferromagnetic order induced solely by an electric field was shown with spatial resolution as shown in the Figure 6 a and b. This experiment revealed that by using a reasonable voltage, the magnetic state of BiFeO<sub>3</sub> thin films could be locally modified. A change in the ferroelectric domain state induced by piezoresponse force microscopy tip poling was followed by a change in the antiferromagnetic domain state. Later, Chu and coworkers [102] engineered a device based on a ferromagnetic CoFe dot magnetically coupled to the multiferroic thin film. Using an in-plane electric field, the magnetization of the CoFe dot could be reversibly rotated by 90° in-plane at room temperature, see Figure 6 c and d. This CoFe layer magnetization reversible change was attributed to interfacial coupling between the ferromagnetic moment and CoFe and the weak ferromagnetic behavior in the BiFeO<sub>3</sub> thin film [6,18]. In a 71° stripe-like domain BiFeO<sub>3</sub> thin film, capped with 2,5 nm thick CoFe ferromagnetic layer, the one to one matching of the ferromagnetic domain and the multiferroic domains in BiFeO<sub>3</sub> was shown using photoemission electron microscopy (PEEM) [99] and scanning electron microscopy with spin polarization analysis (SEMPA) [97,103,104]. The ferromagnetic moment in the CoFe layer aligns with the BiFeO<sub>3</sub> canted moment at the scale of a single domain [97]. In each BiFeO<sub>3</sub> ferroelectric domain, the canted moment, giving rise to the weak ferromagnetic behavior lies in the perovskite (111) plane, in a direction perpendicular to the ferroelectric polarization direction [18]. In the particular case of the 71° stripe domain pattern, this corresponds to in-plane 90° change from one domain to another of both the canted moment and polarization projection onto the (001) surface, as experimentally shown by SEMPA imaging [97] and in Figure 6 e. One can electrically change the polarization direction, this is accompanied with a reorientation of the canted moment direction and therefore, an electrically induced rotation or reversal of the CoFe magnetization can be expected. The actual evidence of a room temperature in-plane electric field induced magnetization reversal was finally

achieved using a stripe-like domain engineered BiFeO<sub>3</sub>/CoFe device. The Co<sub>0.9</sub>Fe<sub>0.1</sub> alloy composition choice leads to minimal magnetostriction coefficient and the magnetic coupling is lost when inserting a non-magnetic but strained intermediate SrTiO<sub>3</sub> 2 nm thick layer [99]. Here, the understanding of the BiFeO<sub>3</sub> domain state during the switching process was a critical step. The net magnetization reversal is based on local 90° rotations summing up to a net 180° change in stripe domain configuration. In each domain, the polarization and therefore the canted moment projection rotates locally by 90° with the applied in-plane electric field. The particular stripe-domain state is a necessity to favor a coherent switching and the resulting net reversal. In the stripe-domain pattern, the neighboring multiferroic domains are indeed driving the reversal switching mechanism [99]. Further investigation of the switching mechanism [105] led to the ability to apply the switching electric field through the multiferroic layer in order to reduce the voltage to 7 V and reverse the ferromagnetic state locally [100], as shown in the Figure 6 f and g.



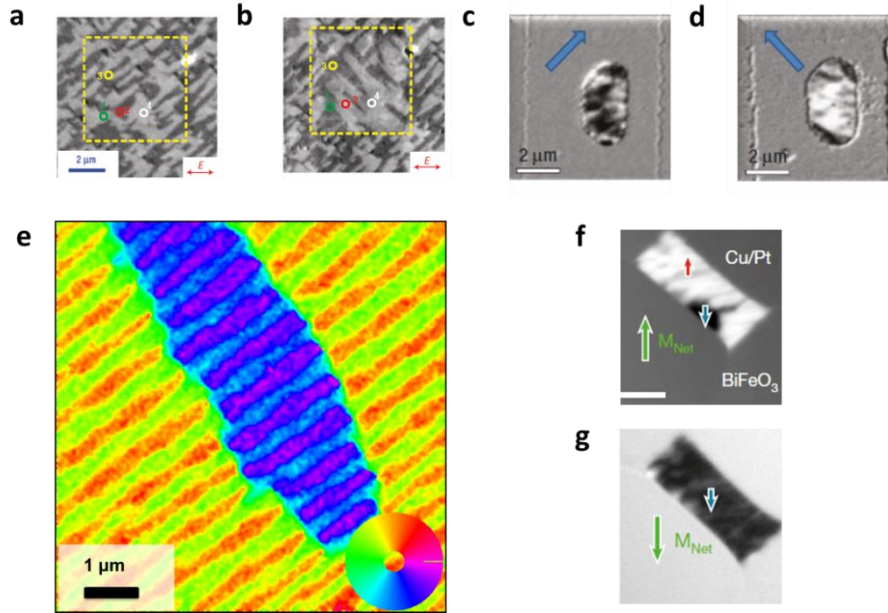


Figure 6. Electric field induced magnetization reversal. a-b) The antiferromagnetic state of  $\text{BiFeO}_3$  thin film can be electrically altered as shown by PEEM images of the as-grown a) state and after application of local voltage in the indicated box in b). Reprinted by permission from Macmillan Publishers Ltd: Nature Materials from [101] copyright 2006. c-d) Using an in-plane electric field the magnetization of a CoFe dot can be rotated by  $90^\circ$  as evidenced by XMCD PEEM in the as grown c) and switched state d). The arrow indicates the net magnetization direction Reprinted by permission from Macmillan Publishers Ltd: Nature Materials from [102] Copyright 2008. e) SEMPA image of a CoFe layer deposited on  $71^\circ$  stripe domain  $\text{BiFeO}_3$  layer. Reprinted figure with permission from [97] Copyright 2013 by the American Physical Society. f,g) XMCD PEEM images in the as grown state f) and after application of an out-of plane electric field g). The local and net magnetization directions are given by the short and long arrows, respectively. The scale bar is  $2 \mu\text{m}$ . Reprinted by permission from Macmillan Publishers Ltd: Nature from [100]. Copyright 2014.

Here again, understanding the magnetoelectric switching process is the key towards the achievement of the net magnetization reversal. The work dealing with out-of-plane capacitor heterostructures revealed that, in this particular orientation and domain state, the direct out-of-plane  $180^\circ$  ferroelectric switch does not exist. In each domain, the switching consists of two successive sub ferroelectric polarization switching events, (i.e.  $71^\circ$  and  $109^\circ$  or  $109^\circ$  and  $71^\circ$ , all leading to the net reversal). The equivalent successive  $90^\circ$  canted moment projection rotations in the  $\text{BiFeO}_3$  film is followed by the reversal of the CoFe ferromagnetic dot deposited on top, at the scale of the single multiferroic domain. This out-of-plane switching process has been confirmed by further ferromagnetic resonance based studies. In these heterostructures indeed, the electrically induced parallel or anti parallel relative orientation of the CoFe

and the underlying canted moment direction in the BiFeO<sub>3</sub> layer give rise to ferromagnetic resonance field shifts [106].

In BiFeO<sub>3</sub> based devices, using an in-plane or an out-of-plane electric field configuration, electrically induced magnetization reversal have only been observed in the particular BiFeO<sub>3</sub> 71° stripe domain configuration. Current state of research is now evolving towards the investigation of ferroelectric switching events in other thin BiFeO<sub>3</sub> film orientations and a less challenging domain state requirements for future device design [107].

### **3. The role of ferroic domains and domain imprint**

In multiferroic heterostructures, electrical modifications of a ferromagnetic state happen at the ferroelectric domain scale. Therefore the ferroelectric domain architecture will influence the heterostructure magnetoelectric behavior. The role of the ferroelectric domains, the control on their anisotropy and the related switching mechanism are emphasized in this section. In artificial multiferroic heterostructures, small domain sizes and the buried configuration of the ferroelectric layer lead to challenging observation of domain imprints.

#### *3.1 Ferroelectric domain engineering*

For tetragonal ferroelectric thin films, i. e. PZT or BaTiO<sub>3</sub>, the strong correlation between epitaxial strain and the polar distortion usually results in single domain state ferroelectric layers. The progress in oxide growth techniques and the development of single crystal substrate manufacture allows engineering the strain state in thin films and therefore, the domain configuration in ferroelectric thin films can be controlled [19,108]. Pioneering theory and experimental work dealing with ferroelectric thin film behavior under epitaxial stress evidenced the potential of epitaxial strain as a new degree of freedom. It has been shown by combined phase field simulation and experimental techniques that indeed strain can lead to polarization tuning, drastic changes in Curie temperature [109,110,111,112] and, more recently, ferroelectric switching event selectivity [113,114].

*The substrate vicinity;* Chu and coworkers demonstrated the ability to modify the ferroelectric domain state of the model multiferroic thin film system BiFeO<sub>3</sub> using the relevant substrate orientation and surface state [115]. It was also shown that for the tetragonal ferroelectric PZT, for a given strain state, the substrate step edges can correspond to preferential nucleation sites for ferroelectric domains [116]. The orientation of the BiFeO<sub>3</sub> ferroelectric domains could also be controlled by the substrate surface

state. From the symmetry allowed 8 possible  $\langle 111 \rangle$  polar axes directions, the number of ferroelectric variants could be tuned to a single domain state, a two ferroelectric variants or four ferroelectric variants configuration depending on the cubic perovskite  $\text{SrTiO}_3$  substrate (111), (110) or (001) orientation, respectively, see Figure 7 a, b, c and d. A substrate orientation dependent PZT thin film study [114], revealed that the domain state as well as the nature of ferroelectric ferroelastic switching events could be controlled by careful selection of the ferroelectric thin film crystalline orientation, see Figure 7e, f and g. Furthermore, the ferroelectric domain degeneracy can be suppressed by changing the substrate miscut angle, going from complex domain architectures to a single domain state with increasing miscut angle [115]. More recently the deterministic control of  $\text{BiFeO}_3$  thin films out-of-plane polarization direction using different substrate buffer chemical termination was shown [117].

*In-plane strain anisotropy induced by the substrate;* The use of orthorhombic scandate substrates opened new avenues towards transferring anisotropic architecture in ferroelectric domain states [97,99]. Among them,  $\text{DyScO}_3$  is the most commonly used. In the (110) plane, a pseudo-cubic unit cell can be defined [118] with a slight anisotropy in in-plane lattice parameter  $a_1=3.951\text{\AA}$  and  $a_2=3.946\text{\AA}$  [119]. This anisotropic in-plane strain results in an orientation dependent epitaxial stress into the film and therefore into an anisotropic domain orientation. Its use for tailoring multiferroic domain is now established. More recently it was used in order to control the orientation in tetragonal ferroelectrics such as PZT [120], see Figure 7 h.

*Ferroelectric flux-closure domain pattern;* In some particular PZT based heterostructures the strain state of the ferroelectric film allows the generation of ferroelectric flux-closure domain pattern [121,122]. Resulting from recent efforts for higher control on domain distribution in heterostructures and superlattices, the theory predicted [123,124,125] flux-closure domain pattern corresponds to a macroscopic polarization rotation within the thin film thickness. The flux-closure domains are promising towards future nanoelectronics applications since their low dimensional finite ferroelectric structure suggests high density information storage potential [123].

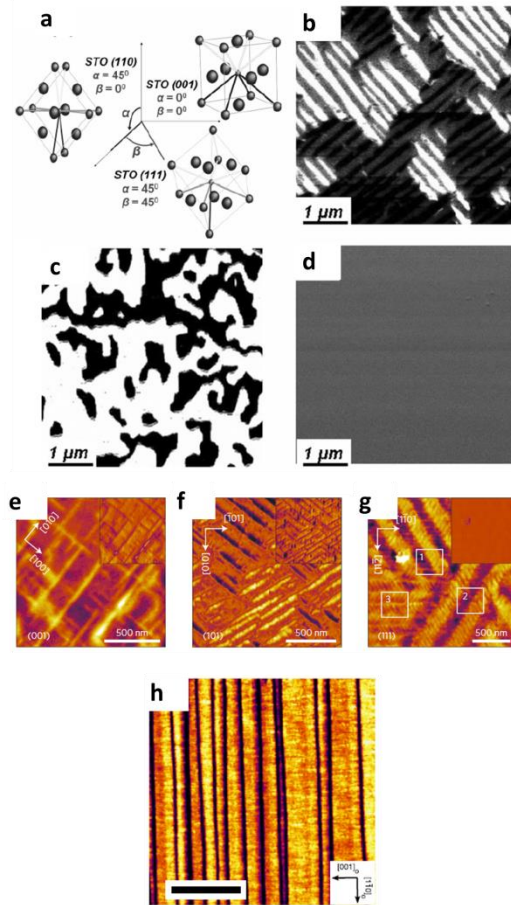


Figure 7. Ferroelectric domain engineering. a-d) The number of  $\text{BiFeO}_3$  ferroelectric variants can be controlled by the substrate orientation. a) orientation of the  $\text{SrTiO}_3$  substrates. b-d)  $\text{BiFeO}_3$  ferroelectric domain structure imaged by Piezoresponse force microscopy on (001), (110) and (111) oriented  $\text{SrTiO}_3$  substrate, respectively. From [115] reproduced with permission (copyright 2007 Wiley-VCH Verlag GmbH & Co. KGaA). e-g) Piezoresponse force microscopy of a PZT thin film grown on  $\text{SrRuO}_3$  buffered (001), (101) and (111)  $\text{SrTiO}_3$  substrates, respectively. Reprinted by permission from Macmillan Publishers Ltd: Nature Communications from [114]. Copyright 2014. h) Piezoresponse force microscopy of a PZT thin film grown on  $\text{SrRuO}_3$  buffered (110) oriented  $\text{DyScO}_3$  substrate. The scale bar is  $1 \mu\text{m}$ . Reprinted by permission from Macmillan Publishers Ltd: Nature Communications from [120]. Copyright 2014.

### 3. 2 Strain induced polarity

Strain acts on the ferroic state, but, in the search for new multiferroics, the idea that strain could be used to induce a polar order was also suggested. The first evidence of strain induced polar state was shown on  $\text{SrTiO}_3$  thin films. This material is known to be an incipient ferroelectric down to 0 K. In 2004, using time

resolved confocal optical microscopy, the ferroelectric response of a biaxially strained SrTiO<sub>3</sub> film grown on DyScO<sub>3</sub> was shown [126]. It was also observed that strain can result in a ferroelectric Curie temperature shift of hundreds of degrees and lead to room temperature ferroelectricity in SrTiO<sub>3</sub>. Later, using a combination of optical second harmonic generation, piezoresponse force microscopy, see Figure 8a, and phase field modeling, the multiferroic character of the SrTiO<sub>3</sub> films was further demonstrated (i.e. ferroelectric and ferroelastic) [127]. This concept was pursued towards the achievement of a strong ferroelectric ferromagnetic multiferroic behavior observation in EuTiO<sub>3</sub> thin films. Following the theoretical prediction [128], EuTiO<sub>3</sub> thin films were grown under 1.1% biaxial strain and the combined induced ferromagnetic, ferroelectric state was confirmed by careful magneto optic Kerr rotation and optical second harmonic generation [129], see Figure 8b. More recently, the experimental evidence of an epitaxial strain induced polar state was shown in SrMnO<sub>3</sub> thin film [130]. This strain induced polar state was predicted by first principles calculations [131]. Interestingly, it was additionally found in this system a correlation between strain and oxygen vacancy ordering. The formation of oxygen vacancies being dependent on the strain state of the thin film [132], their increased concentration is expected in the strained SrMnO<sub>3</sub> layer. Experimental results show the coupling between these oxygen vacancies and the polar domain walls [130]. The combined effect leads to peculiar conductance pattern, showing polar domains delimited by insulating oxygen vacancies rich walls, see Figure 8c.

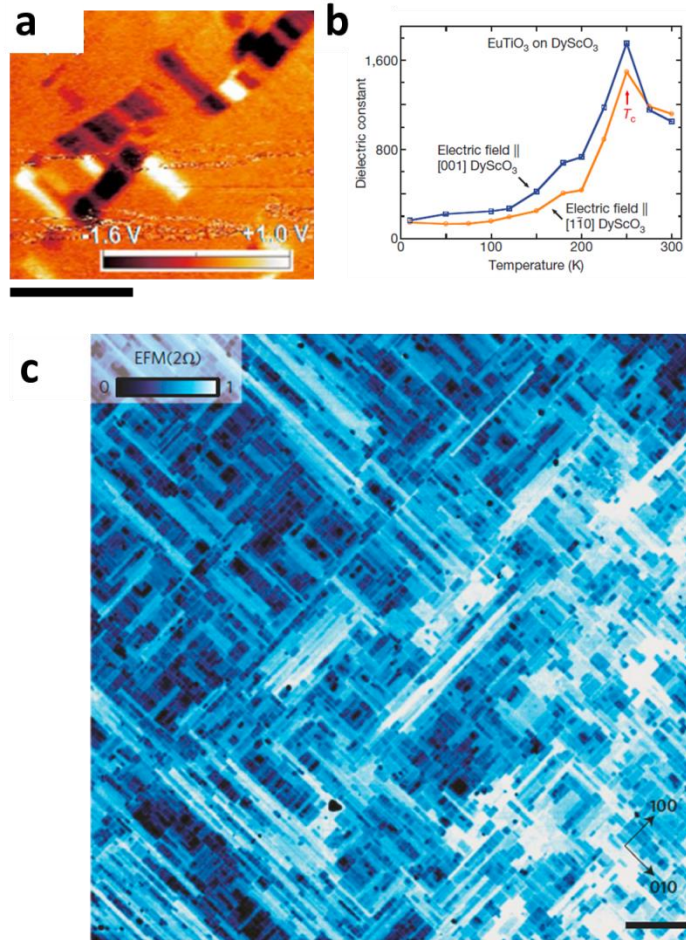


Figure 8. Strain induced polar states. a) Ferroelectric domains observed by piezoresponse force microscopy on  $\text{SrTiO}_3$  thin film. Scale bar is  $10\ \mu\text{m}$ . Reprinted figure with permission from [127] Copyright 2006 by the American Physical Society. b) Dielectric constant as function of temperature, showing a ferroelectric Curie temperature of 250 K for a ferromagnetic  $\text{EuTiO}_3$  thin film. Reprinted by permission from Macmillan Publishers Ltd: Nature from [129]. Copyright 2010. c) Conductance pattern measured on a polar  $\text{SrMnO}_3$  strained thin film. Scale bar is  $5\ \mu\text{m}$ . Reprinted by permission from Macmillan Publishers Ltd: Nature Nanotechnology from [130]. Copyright 2015.

### 3.3 Ferroic domain imprint in multiferroic heterostructures

It is now established that, in multiferroic heterostructures, the magnetoelectric behavior is determined by the interfaces (charge, strain, or magnetism). In ferroelectric ferromagnetic heterostructures, another critical parameter is the ferroelectric domain configuration and its influence on the adjacent ferromagnetic layer. The simultaneous observation of ferroelectric and ferromagnetic domains is

however rather challenging at the nanoscale. In bulk single phase multiferroics, large multiferroic domains can be accessed directly using optical techniques [133], but in artificial multiferroic heterostructures, the ferroelectric layer is buried below the magnetic film, and its nanoscale domain architecture is then no longer accessible using conventional contact scanning probe techniques. Experimental observation of buried ferroelectric state are usually limited to the out-of-plane polarization contribution [134,135,136].

The so called ferroelectric imprint in the ferromagnetic layer can originate from the magnetostriction coupling and has mainly been observed in bulk-ferroelectric-based heterostructures [41,137]. Using magneto optic Kerr effect (MOKE) or X-ray photoemission electron microscopy (X-PEEM) the local matching of the ferroelectric (in-plane and out-of-plane) macroscopic ordering and transfer in the ferromagnet layer was shown [138]. The ferroelectric imprint determines the macroscopic behavior of the heterostructures, i. e. magnetic anisotropy and coercivity but also and most interestingly its behavior under electric field, see Figure 9a. For instance, in the BaTiO<sub>3</sub>/CoFe, ferromagnetic walls motion was electrically induced [43].

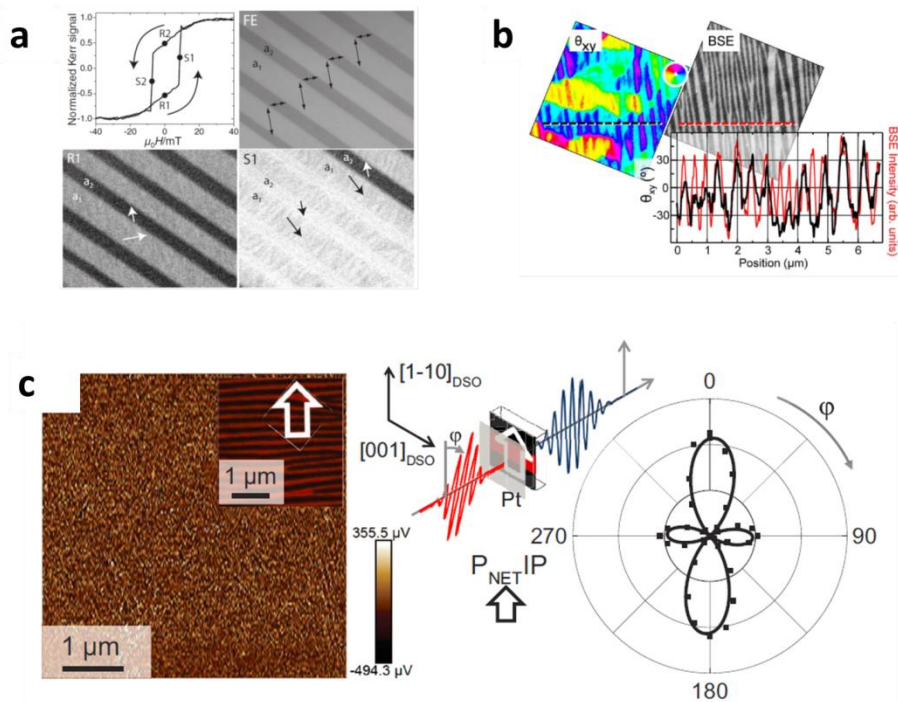


Figure 9. Ferroelectric domain imprint into strong ferromagnets. a) Magnetic hysteresis loop obtained by magneto optic Kerr effect and corresponding images of the underlying ferroelectric state and ferromagnetic contrast in CoFe layer grown on BaTiO<sub>3</sub> ferroelectric crystal. The images areas are 30x40μm<sup>2</sup>. From [41] reproduced with permission (copyright 2011 Wiley-VCH Verlag GmbH & Co. KGaA). b) Scanning electron microscopy with polarization analysis and electron backscattered contrast showing local matching of the ferromagnetic and ferroelectric domains in BiFeO<sub>3</sub>/CoFe heterostructure. Reprinted with permission from [104]. Copyright 2014, AIP Publishing LLC. c) Optical second harmonic analysis of multiferroic BiFeO<sub>3</sub> thin film domain state capped with a 4 nm thick Pt electrode. In c) no contrast is visible using Piezoresponse force microscopy but the net in-plane ferroelectric direction is still accessible using optical second harmonic generation light polarization analysis. From [143] reproduced with permission (copyright 2015 Wiley-VCH Verlag GmbH & Co. KGaA).

Another system in which the one-to-one matching of multiferroic ferroelectric and ferromagnetic domains has been locally shown is the BiFeO<sub>3</sub>/CoFe heterostructure. In this particular case, the BiFeO<sub>3</sub> imprint is attributed to a magnetic interfacial coupling between the multiferroic domain and the CoFe [97,105]. Using magnetic force microscopy, the strength of the magnetic coupling between the multiferroic thin film and the ferromagnetic layer could be estimated and an in-plane effective coupling field of order 10 mT is derived from simulations [97]. The macroscopic manifestation of this strong



interfacial coupling is a CoFe layer enhanced coercivity, a uniaxial magnetic anisotropy and a magnetic easy axis aligning along the underlying net in-plane polarization. Thanks to this one-to-one domain matching, local ferroelectric switching events correspond to local magnetization switchings and therefore, a net polarization reversal was followed by a net magnetization reversal [99]. Scanning electron microscopy with polarization analysis is a powerful tool for nanoscale in-plane magnetization observation, using the backscattered electron imaging contrast, the underlying ferroelectric state can also be accessed [104]. However, this imaging technique is not suitable after voltage application. Recent work dealing with the optical probing of ferroelectric domain engineering in BiFeO<sub>3</sub> thin films showed that optical second harmonic is an efficient way to probe the out-of-plane and in-plane component of the domain architecture in multiferroic and ferroelectric [139,140,141,142] bulk and thin films even in a buried configuration [143]. The BiFeO<sub>3</sub> thin film ferroelectric domain architecture was indeed optically determined before and after local voltage application and could even be accessed through a 4 nm thick conducting Pt top electrode.

#### **4. Multiferroic heterostructures for spintronics**

In the following the different device concepts, developed among the advances in magnetoelectric multiferroic heterostructures, will be described. Taking advantage of the achievement dealing with voltage induced magnetization reversal or magnetic domains and domain wall motions, low energy consuming non-volatile magnetic memories, magnetic nanologics or memristors can be foreseen.

##### *4.1 Magnetoelectric multiferroic memories*

The concept of magnetoelectric memories [144], see Figure 10 a, was developed with the revival of multiferroics magnetoelectrics [10]. Magnetoelectric memories have to be distinguished from multiferroic memories. In multiferroic magnetic memories, the magnetoelectric coupling is not considered and a bit can be independently written in the ferroelectric or magnetic order parameter [145,146]. The first multiferroic memory was experimentally designed using a multiferroic tunnel junction [145]. The electron tunneling could be electrically and magnetically tuned individually and four different resistance states were achieved on the same tunnel junction. This introduces the advantage of data storage density increased capacity [146]. Further investigation dealing with the presence of a ferroelectric component in a tunnel junction revealed high potential for strain and magnetic field detection applications [24,78,147,148]. In the case of the multiferroic magnetoelectric memories, a strong coupling between the two order parameters (magnetic and electric) is necessary. The non-volatile

magnetic state is electrically written. The experimental realization of a magnetoelectric memory allowing for magnetic reading and electric writing was performed in a multiferroic magnetoelectric BiFeO<sub>3</sub> based heterostructure by Heron and coworkers [100]. By depositing a spin valve heterostructure coupled to the multiferroic magnetoelectric BiFeO<sub>3</sub> layer, the magnetoresistance state was reversibly changed using solely a 7 V pulse. The corresponding energy consumption to electrically reverse the magnetic bit was quantified and estimated to be an order of magnitude lower than in an optimized spin torque device [100,149,150]. Efforts are now shifting into the device life time improvement. At the metal/oxide interface, defects such as oxygen vacancies can accumulate and deteriorate the magnetoelectric interface quality [100]. Using the same out-of-plane voltage application, the electrically induced magnetization reversal was recently observed in hundreds of cycles [106].

#### *4.2 Multiferroics in magnetic nanologic*

In nanologics, the nearest-neighbor dipole field coupling between neighboring nanomagnets is used to propagate and modify the binary information. The experimental use of magnetically bistable nanodots to encode a bit of information has been first demonstrated in 2006 [151]. An input magnetic dot is driving a chain of dipolar field coupled nanodots. In between two inputs, the chain is “clocked”, i. e., a magnetic field is applied to reset the magnetic chain. Nanomagnet logics present high interest for information processing since the energy necessary to manipulate nanomagnetic chains is predicted to be minimal [152]. The current limitation for energy efficient use of nanologic is the need of external magnetic field for clocking the circuits. Recently, it was shown that spin hall effect could be used to set the magnetic nanodots into a metastable state, therefore, spin orbit torque was suggested as potential replacement of the external magnetic field [153], see the sketch in Figure 10 b. The interest in magnetoelectric multiferroic for nanologic resides in the possibility to electrically drive the magnet chain, i. e. set electrically the magnetic state of the input magnetic nanodot (Figure 10 b), and therefore achieve ultra-low power dissipation [154,155]. However, the illustration in Figure 10 b, involves metallic systems, the use of magnetoelectric coupling to control the input dot would require efforts in device designing towards the combination of spin hall effect and oxide magnetoelectric compounds. Buzzi and coworkers have demonstrated a 90° electric field-induced uniform magnetization rotation in single domain submicron ferromagnetic dots [48]. This corresponds to a first step towards the achievement of electrical control of single domain magnetic dots. So far, the electric field induced magnetization reversal was limited to micron scale device with specific multiferroic domain configuration [99,100,106]. Combining

this ability down to the nanoscale with spin orbit torque clocking would lead to nanologic operations in absence of external magnetic field.

#### *4.3. Multiferroic Memristor*

The memory resistor (memristor) is now considered as the fourth circuit building element together with the resistor, inductor and capacitor [156]. Memristors are continuously tunable resistors. Several mechanisms involving conducting filament formation or oxygen vacancies migration are developed in order to describe the resistive switching process [157]. This voltage induced resistance switching has been observed in a wide variety of transition metal oxides [158] and more recently in ferroelectric based heterostructures [134]. In 2009, the concept of spintronic memristor was developed [159]. Its principle is based on spin torque induced domain wall motion resulting in tunable magnetoresistance in spin valve heterostructures. The use of spin polarized current to induce domain wall motion is already considered for the previously mentioned race track memory device [37]. Recent progress in device geometry allows the increase of current induced domain wall motion efficiency with the vertical current injection geometry [160,161].

In the push for low energy consumption spintronics, the insertion of magnetoelectric multiferroics into the magnetic memristor architecture would be a step forward, leading to voltage induced tunable magnetoresistance. The multiferroic magnetoelectric device is based on the electrically tunable multiferroic imprint into a ferromagnetic electrode as described in the Figure 10 c. Instead of spin current, the domain wall position which sets the device magnetoresistance is given by the underlying multiferroic domain wall location. This concept is then limited by the ability to deterministically control a ferroelectric individual domain wall movement. In their recent work Mc Gilly and coworkers [162] demonstrated that such a control could be established in ferroelectric thin films by tuning the applied voltage pulses. The ferroelectric domain wall velocity can further be tuned by epitaxial strain [163]. The high dynamic potential of multiferroic heterostructures for electric field induced magnetic domain wall motion has been shown [164]. Moreover, a new concept of ferroelectric domain wall diode is being developed in order to allow chains of ferroelectric domains or domain walls to travel in a deterministic fashion [165].

All these recent developments are paving the way of multiferroic magnetoelectric memristors in which the domain imprint into the ferromagnet will be deterministically controlled heading towards continuous

electrically induced resistance changes without energy consuming spin current injection. This would consist into a robust memory element with minimal energy dissipation.

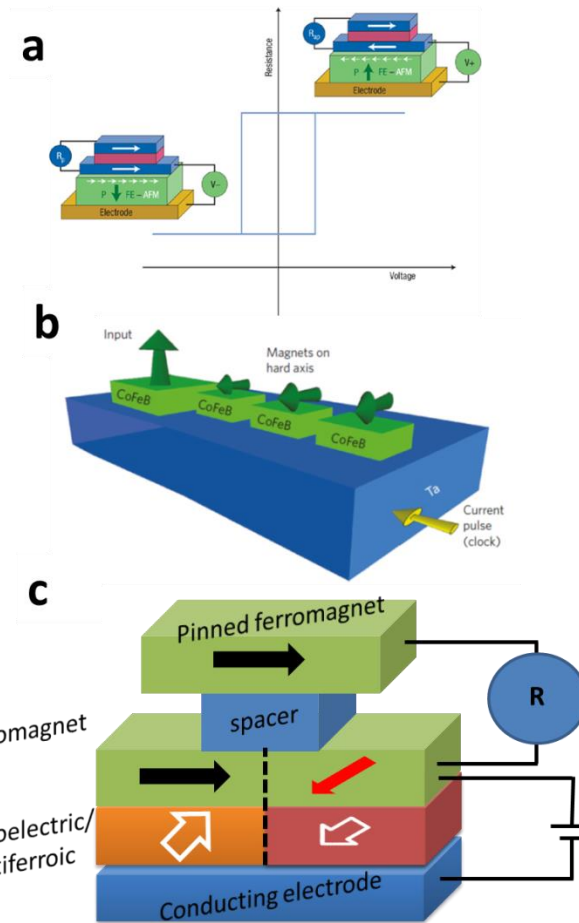


Figure 10. Multiferroic heterostructures for spintronics. a) The multiferroic magnetoelectric memory concept consists in inserting a magnetoelectric material in the vicinity of a spin valve heterostructure in order to achieve a resistance change as function of the applied voltage. Reprinted by permission from Macmillan Publishers Ltd: Nature Materials from [144] copyright 2008. b) Schematization of spin Hall effect clocking of CoFeB nanodots. Reprinted by permission from Macmillan Publishers Ltd: Nature Nanotechnology from [153] copyright 2014. c) Multiferroic magnetoelectric memristor concept. The electrically adjustable multiferroic wall position is transferred into the ferromagnetic layer. The magnetoresistance is therefore continuously electrically tunable.

## 5. Future perspectives and concluding remarks

The current achievements towards energy efficient spintronics using magnetoelectric multiferroic heterostructures have been reviewed. We will now discuss the remaining challenges and limitations regarding the insertion of multiferroics into spintronics devices. In order to be competitive with other spin polarized current based technologies, a better understanding of magnetoelectric switching and interfacial coupling is needed. Simultaneous detection of ferroelectric and ferromagnetic state is a necessity in order to gain knowledge on the robustness and on the dynamics of multiferroic devices.

### 5.1 Towards single domain switching.

As described in the previous sections, the ability to electrically reverse a single domain magnet is of high interest for nanosized spintronics [154,155]. Furthermore, the progress in device design is now pushing the need towards single magnetic wall motion control [37]. In the current state of the art room temperature multiferroic magnetoelectric heterostructures, nanodots magnetic easy axes can be electrically rotated by  $90^\circ$  in-plane [48] and, on the micron scale, a magnetization can be reversed [100]. In order to be competitive with other technologies, magnetoelectric switchings have to be induced using simpler multiferroic domain architecture. The present demonstration of electric field induced magnetization reversal [100,106] relies on the stability of the stripe domain structure under applied voltages [166], therefore, a single domain state is highly needed to provide the required robustness of the switching event. Recent progress in multiferroic thin film analysis revealed that magnetoelectric behavior is preserved on a wide variety of substrates and strain states [17], offering new opportunities for the observation of efficient magnetoelectric switching at room temperature. The development of experimental techniques allowing simultaneous imaging of ferromagnetic and ferroelectric domains [41,104,143] in heterostructures, aiming to the observation of multiferroic domain imprint will also favor advances in the field of electrically induced ferromagnetic wall motion.

### 5.2 Magnetoelectric switching dynamics

A crucial step towards the insertion of multiferroics into spintronics is the determination of magnetoelectric switching dynamics. So far only a few studies are focusing on the electric field induced switching dynamics [167,168]. In bulk magnetoelectrics, the switching dynamics can indeed be incompatible with the device requirements. For instance, in  $\text{MnWO}_4$ , the electric field induced magnetic response change happens on the millisecond time scale [168].

Further investigation of magnetoelectric switching dynamics is therefore needed in order to estimate the real potential of multiferroic magnetoelectric heterostructures. In the out-of-plane voltage application configuration, the room temperature magnetoelectric switching resulting into a net magnetization reversal involves at least two ferroelectric switching steps [100]. This could for instance limit the dynamic of the devices. On the other hand, spin orbit torque based switching have been recently shown to exhibit ultra-fast reversal dynamics [169], with switching pulse width down to 180 picoseconds. The high potential of nanomagnetic chains for ultra-fast logic operation has also recently been revealed [170]. The recent ability to use optical techniques to probe multiferroic switching event [143] in artificial multiferroic heterostructures is a promising step towards the determination of the magnetoelectric switching dynamics.

### **Acknowledgements**

M T thanks G De Luca and N Viart for proofreading of the manuscript, D Meier and K Garello for fruitful and M Fiebig for his valuable insight and financial support. M T also acknowledge the financial support from the SNSF R'Equip Program (No.206021-144988)

## References

- 
- <sup>1</sup> Spaldin N, Fiebig M, 2005 *Science*. **309** 5733
  - <sup>2</sup> Hill N A, 2000 *J. Phys. Chem. B*. **104** 6694
  - <sup>3</sup> Cheong S W, Mostovoy M 2007 *Nat. Mater.* **6** 13
  - <sup>4</sup> Rabe K M, Triscone J M, Ahn C H 2007 *Physics of Ferroelectrics: A modern perspective*. Springer
  - <sup>5</sup> Seshadri R, and Hill N A 2001 *Chem. Mater.* **13**, 2892
  - <sup>6</sup> Wang J, Neaton J B, Zheng H, Nagarajan V, Ogale S B, Liu B, Viehland D, Vaithyanathan V, Schlom D G, Waghmare U V, Spaldin N A, Rabe K M, M. Wuttig M, Ramesh R 2003 *Science* **299**, 1719
  - <sup>7</sup> Fiebig M, Lottermoser Th, Fröhlich D, Goltsev A V, and Pisarev R V 2002 *Nature* **419** 818
  - <sup>8</sup> Kimura T, Goto T, Shintani H, Ishizaka K, Arima T, and Tokura Y 2003 *Nature* **426** 55
  - <sup>9</sup> Kenzelmann M, Harris A B, Jonas S, Broholm C, Schefer J, Kim S B, Zhang C L, Cheong S W, Vajk O P, and Lynn J W 2005 *Phys. Rev. Lett.* **95** 087206
  - <sup>10</sup> Fiebig M, 2005 *J. Phys. D: Appl. Phys.* **38** R123
  - <sup>11</sup> Eerenstein W, Mathur N D and Scott J F 2006 *Nature* **442** 759
  - <sup>12</sup> Scott J F *NPG Asia Materials* 2013 **5** e72
  - <sup>13</sup> Rado G T *Phys. Rev. Lett.* 1964 **13** 335
  - <sup>14</sup> Trassin M, Viart N, Versini G, Barre S, Pourroy G, Lee J H, Jo W, Dumesnil K, Dufour C, and Robert S 2009 *J. Mater. Chem.* **19** 8876
  - <sup>15</sup> Smolenskii A, Chupis I, 1982 *Sov. Phys. Usp.* **25** 475
  - <sup>16</sup> Lebeugle D, Colson D, Forget A, Viret M, Bonville P, Marucco J F, and Fusil S 2007 *Phys. Rev. B* **76** 024116
  - <sup>17</sup> Sando S, Agbelele A, Rahmedov D, Liu J, Rovillain P, Toulouse C, Infante I C, Pyatakov A P, Fusil S, Jacquet E, Carrétéro C, Deranlot C, Lisenkov S, Wang D, Le Breton J M, Cazayous M, Sacuto A, Juraszek J, Zvezdin A K, Bellaiche L, Dkhil B, Barthélémy A, and Bibes M 2013 *Nat. Mater.* **12** 641
  - <sup>18</sup> Ederer C, and Spaldin N A 2005 *Phys. Rev. B* **71** 060401(R)
  - <sup>19</sup> Ramesh R, and Spaldin N A 2007 *Nature Mater.* **6** 21
  - <sup>20</sup> Vaz C A F, and Staub U 2013 *J. Mater. Chem. C* **1** 6731
  - <sup>21</sup> Duan C G, Jaswal S S, and Tsymbal E Y 2006 *Phys. Rev. Lett.* **97** 047201
  - <sup>22</sup> Lahtinen T H E, Framke K J A, and Van Dijken S 2012 *Sci. Rep.* **2** 258
  - <sup>23</sup> Biegalski M D, Dörr K, Kim D H, Christen H M 2010 *Appl. Phys. Lett.* **96** 151905
  - <sup>24</sup> Valencia S, Crassous A, Bocher L, Garcia V, Moya X, Cherifi R O, Deranlot C, Bouzheouane K, Fusil S, Zobelli, Gloter A, Mathur N D, Gaupp A, Abrudan R, Radu F, Barthélémy A, and Bibes M 2011 *Nature Mater.* **10** 753

- 
- <sup>25</sup> Baibich M N, Broto J M, Fert A, Nguyen Van Dau F, Petroff F, Etienne P, Creuzet G, Friederich A, and Chazelas J 1988 Phys. Rev. Lett. **61** 2472
- <sup>26</sup> Binasch G, Grünberg P, Saurenbach F, and Zinn W 1989 Phys. Rev. B **39** 4828(R)
- <sup>27</sup> Ralph D C, and Stiles M 2008 J. Magn. Magn. Mater. **320** 1190
- <sup>28</sup> Myers E B, Ralph D C, Katine J A, Louie R N, Buhrman R A 1999 Science **285** 867
- <sup>29</sup> Zhu J G 2008 Proceedings of the IEEE **96** 1786
- <sup>30</sup> Dyakonov M, and Perel V 1971 Phys. Lett. A **35** 459
- <sup>31</sup> Edelstein V M 1990 Sol. St. Comm. **73** 233
- <sup>32</sup> Garello K, Miron I M, Avci C O, Freimuth F, Mokrousov Y, Blügel S, Auffret S, Boulle O, Gaudin G, and Gambardella P 2013 Nat.Nano. **8** 587
- <sup>33</sup> Miron I M, Gaudin G, Auffret S, Rodmacq B, Schuhl A, Pizzini S, Vogel J, and Gambardella P 2010 Nature Mater. **9** 230
- <sup>34</sup> Liu L, Pai C F, Li Y, Tseng H W, Ralph D C, Buhrman R A 2012 Science **336** 555
- <sup>35</sup> Pai C F, Liu L, Li Y, Tseng H W, Ralph D C, and Buhrman R A 2012 Appl. Phys. Lett. **101** 122404
- <sup>36</sup> Miron I M, Garello K, Gaudin G, Zermatten P J, Costache M V, Auffret S, Bandiera S, Rodmacq B, Schuhl A, and Gambardella P 2011 Nature **476** 189
- <sup>37</sup> Parkin S S P, Hayashi M, and Thomas L 2008 Science **320** 5873
- <sup>38</sup> Shiota Y, Nozaki T, Bonell F, Murakami S, Shinjo T, and Suzuki Y 2012 Nature Mater. **11** 39
- <sup>39</sup> Novosad V, Otani Y, Ohsawa A, Kim S G, Fukamichi K, Koike J, Maruyama K, Kitakami O, and Shimada Y 2000 J. Appl. Phys. **87** 6400
- <sup>40</sup> Wu T, Bur A, Wong K, Zhao P, Lynch C S, Amiri P K, Wang K L, and Carman G P 2011 Appl. Phys. Lett. **98** 262504
- <sup>41</sup> Lahtinen T H E, Tuomi J E, and van Dijken S 2011 Adv.Mater. **23** 3187
- <sup>42</sup> Franke K J A, Lopez Gonzalez D, Hämäläinen S J, and van Dijken S, 2014 Phys. Rev. Lett. **112**, 017201
- <sup>43</sup> Franke K J A, Van de Wiele B, Shirahata Y, Hämäläinen S J, Taniyama T, and van Dijken S 2015 Phys. Rev. X **5** 011010
- <sup>44</sup> Hunter D, Osborn W, Wang K, Kazantseva N, Hattrick-Simpers J, Suchoski R, Takahashi R, Young M L, Mehta A, Bendersky L A, Lofland S E, Wuttig M, and Takeuchi I 2011 Nature Comm. **2** 518
- <sup>45</sup> Williams P I, Lord D G, and Grundy P J 1994 J. Appl. Phys. **75** 5257
- <sup>46</sup> Nan T, Zhou Z, Liu M, Yang X, Gao Y, Assaf B A, Lin H, Velu S, Wang X, Luo H, Chen J, Akhtar S, Hu E, Rajiv R, Krishnan K, Sreedhar S, Heiman D, Howe B M, Brown G J, and Sun N X 2014 Sc. Rep. **4** 3688
- <sup>47</sup> Yang W G, Morley N A, Sharp J, and Rainforth W M 2015 J. Appl. Phys. D: Appl. Phys. **48** 305005



- 
- <sup>48</sup> Buzzi M, Chopdekar R V, Hockel J L, Bur A, Wu T, Pilet N, Warnicke P, Carman G P, Heyderman L J, and Nolting F 2013 *Phys. Rev. Lett.* **111** 027204
- <sup>49</sup> Hockel J L, Bur A, Wu T, Wetzlar K P, Carman G P 2012 *Appl. Phys. Lett.* **100** 022401
- <sup>50</sup> Wu T, Zhao P, Bao M, Bur A, Hockel J L, Wong K, Mohanchandra K P, Lynch C S, Carman G P 2011 *J. Appl. Phys.* **109** 124101
- <sup>51</sup> Wu T, Bur A, Zhao P, Mohanchandra K P, Wong K, Wang K L, Lynch C S, and Carman G P 2011 *Appl. Phys. Lett.* **98**, 012504
- <sup>52</sup> Feng M, Wang J J, Hu J M, Wang J, Ma J, Li H B, Shen Y, Lin Y H, Chen L Q, and Nan C W 2015 *Appl. Phys. Lett.* **106** 072901
- <sup>53</sup> Liu M, Li S, Zhou Z, Beguhn S, Lou J, Xu F, Lu T J, and Sun N X 2012 *J. Appl. Phys.* **112** 063917
- <sup>54</sup> Hockel J L, Wu T, and Carman G P *J. Appl. Phys.* **109** 064106
- <sup>55</sup> Herklotz A, Biegalski M D, Christen H M, Guo E J, Nenkov K, Rata A D, Schultz L, and Dörr K 2014 *Phil. Trans. R. Soc. A* **372** 20120441.
- <sup>56</sup> Biegalski M D, Dörr K, Kim D H, and Christen H M 2010 *Appl. Phys. Lett.* **96**, 151905
- <sup>57</sup> Yu P, Chu Y H, and Ramesh R 2012 *Materials Today* **15** 320
- <sup>58</sup> Wang J J, Hu J M, Ma J, Zhang J X, Chen L Q, and Nan C W 2014 *Sc. Rep.* **4** 7507
- <sup>59</sup> Duan C G, Velev J P, Sabirianov R F, Zhu Z, Chu J, Jaswal S S, and Tsymbal E Y 2008 *Phys. Rev. Lett.* **101** 137201
- <sup>60</sup> Duan C G, Jaswal S S, and Tsymbal E Y 2006 *Phys. Rev. Lett.* **97** 047201
- <sup>61</sup> Duan C G, Velev J P, Sabirianov R F, Mei W N, Jaswal S S, and Tsymbal E Y 2008 *Appl. Phys. Lett.* **92** 122905
- <sup>62</sup> Niranjana M K, Duan C G, Jaswal S S, and Tsymbal E Y 2010 *Appl. Phys. Lett.* **96** 222504 (2010)
- <sup>63</sup> Zhang S 1999 *Phys. Rev. Lett.* **83** 640
- <sup>64</sup> Nozaki T, Shiota Y, Shiraishi M, Shinjo T and Suzuki Y 2010 *Appl. Phys. Lett.* **96** 022506
- <sup>65</sup> Maruyama T, Shiota Y, Nozaki T, Ohta K, Toda N, Mizuguchi M, Tulapurkar A A, Shinjo T, Shiraishi M, Mizukami S, Ando Y, and Suzuki Y 2009 *Nat Nano.* **4** 158
- <sup>66</sup> Ikeda S, Miura K, Yamamoto H, Mizunuma K, Gan H D, Endo M, Kanai S, Hayakawa J, Matsukura F, and Ohno H 2010 *Nat. Mater.* **9** 721
- <sup>67</sup> Wang W G, Li M, Hageman S, and Chien C L 2012 *Nat. Mater.* **11** 64
- <sup>68</sup> Mardana A, Ducharme S, and Adenwalla S 2011 *Nano Lett.* **11** 3862
- <sup>69</sup> Jedrecy N, von Bardeleben H J, Badjeck V, Demaille D, Stanescu D, Magnan H, and Barbier A 2013 *Phys. Rev. B* **88** 121409(R)
- <sup>70</sup> Jia C L, Wei T L, Jiang C J, Xue D S, Sukhov A, and Berakdar J 2014 *Phys. Rev. B* **90** 054423
- <sup>71</sup> Ohno H, Chiba D, Matsukura F, Omiya T, Abe E, Dietl T, Ohno Y, and Ohtani K 2000 *Nature* **408** 944

- 
- <sup>72</sup> Chiba D, Yamanouchi M, Matsukura F, and Ohno H 2003 *Science* **301** 943
- <sup>73</sup> Sawicki M, Chiba D, Korbecka A, Nishitani Y, Majewski J A, Matsukura F, Dietl T, and Ohno H 2010 *Nat. Phys.* **6** 22
- <sup>74</sup> Matsukura F, Tokura Y, and Ohno H 2015 *Nat. Nano.* **10** 209
- <sup>75</sup> Molegraaf H J A, Hoffman J, Vaz C A F, Gariglio S, van der Marel D, Ahn C H, Triscone J M 2009 *Adv. Mater.* **21** 3470
- <sup>76</sup> Ramirez A P 1997 *J. Phys.: Condens. Matter* **9** 8171
- <sup>77</sup> Lu H, George T A, Wang Y, Ketsman I, Burton J D, Bark C W, Ryu S, Kim D J, Wang J, Binek C, Dowben P A, Sokolov A, Eom C B, Tsymbal E I, and Gruverman A 2012 *Appl. Phys. Lett.* **100** 232904
- <sup>78</sup> Pantel D, Goetze S, Hesse D, and Alexe M 2012 *Nat. Mater.* **11** 289
- <sup>79</sup> Preziosi D, Alexe M, Hesse D, and Salluzzo M 2015 *Phys. Rev. Lett.* **115** 157401
- <sup>80</sup> Yi D, Liu J, Okamoto S, Jagannatha S, Chen Y C, Yu P, Chu Y H, Arenholz E, and Ramesh R 2013 *Phys. Rev. Lett.* **111** 127601
- <sup>81</sup> Kudrnovský J, Drchal V, and Turek T 2015 *Phys. Rev. B* **91** 014435
- <sup>82</sup> Lee Y, Liu Z Q, Heron J T, Clarkson J D, Hong J, Ko C, Biegalski M D, Aschauer U, Hsu S L, Nowakowski M E, Wu J, Christen H M, Salahuddin S, Bokor J B, Spaldin N A, Schlom D G, and Ramesh R 2015 *Nat. Comm.* **6** 5959
- <sup>83</sup> Cherifi R O, Ivanovskaya V, Phillips L C, Zobelli A, Infante I C, Jacquet E, Garcia V, Fusil S, Briddon P R, Guiblin N, Mougín A, Ůnal A A, Kronast F, Valencia S, Dkhil B, Barthélemy A, and Bibes M 2014 *Nat. Mater.* **13** 345
- <sup>84</sup> Marti X, Fina I, Frontera C, Liu J, Wadley P, He Q, Paull R J, Clarkson J D, Kudrnovský J, Turek I, Kuneš J, Yi D, Chu J H, Nelson C T, You L, Arenholz E, Salahuddin S, Fontcuberta J, Jungwirth T, and Ramesh R 2014 *Nat. Mater.* **13** 367
- <sup>85</sup> Laukhin V, Skumryev V, Marti X, Hrabovsky D, Sanchez F, Garcia-Cuenca M V, Ferrater C, Varela M, Luders U, Bobo J F, and Fontcuberta J 2006 *Phys. Rev. Lett.* **97** 227201
- <sup>86</sup> Fiebig M, Lottermoser Th, Fröhlich F, Goltsev A V, and Pisarev R V 2002 *Nature* **419** 818
- <sup>87</sup> Martin L W, Chu Y H, Zhan Q, Ramesh R, Han S J, Wang S X, Warusawithana M, and Schlom D G 2007 *Appl. Phys. Lett.* **91** 172513
- <sup>88</sup> Allibe J, Fusil S, Bouzehouane K, Daumont C, Sando D, Jacquet E, Deranlot C, Bibes M, and Barthélemy A 2013 *Nano Lett.* **12** 1141
- <sup>89</sup> Matzen S, Fusil S 2015 *C. R. Physique* **16** 227
- <sup>90</sup> Martin L W, Chu Y H, Holcomb M B, Huijben M, Yu P, Han S J, Lee D, Wang S X, and Ramesh R 2008 *Nano Lett.* **8** 2050
- <sup>91</sup> Privratska J, and Janovec V 1997 *Ferroelectrics* **204** 321

- 
- <sup>92</sup>Cruz M P, Chu Y H, Zhang J X, Yang P L, Zavaliche F, He Q, Shafer P, Chen L Q, and Ramesh R 2007 Phys. Rev. Lett. **99** 217601
- <sup>93</sup> Yu P, Lee J S, Okamoto S, Rossell M D, Huijben M, Yang C H, He Q, Zhang J X, Yang S Y, Lee M J, Ramasse Q M, Erni R, Chu Y H, Arena D A, Kao C C, Martin L W, and Ramesh R 2010 Phys. Rev. Lett. **105** 027201
- <sup>94</sup>Wu S M, Cybart S A, Yu P, Rossell M D, Zhang J X, Ramesh R, and Dynes R C 2010 Nat. Mater. **9** 756
- <sup>95</sup> Wu S M, Cybart S A, Yi D, Parker J M, Ramesh R, and Dynes R C 2013 Phys. Rev. Lett. **110** 067202
- <sup>96</sup> Huijben M, Yu P, Martin L W, Molegraaf H J A, Chu J H, Holcomb M B, Balke N, Rijnders G, and Ramesh R 2013 Adv. Mater. **25** 4739
- <sup>97</sup> Trassin M, Clarkson J D, Bowden S R, Liu J, Heron J T, Paull R J, Arenholz E, Pierce D T, and Unguris J 2013 Phys. Rev. B **87** 134426
- <sup>98</sup> Chu Y H, Zhao T, Cruz M P, Zhan Q, Yang P L, Martin L W, Huijben M, Yang C H, Zavaliche F, Zheng H, and Ramesh R 2007 Appl. Phys. Lett. **90** 252906
- <sup>99</sup>Heron J T, Trassin M, Ashraf K, Gajek M, He Q, Yang S Y, Nikonov D E, Chu Y H, Salahuddin S, and Ramesh R 2011 Phys. Rev. Lett. **107** 217202
- <sup>100</sup>Heron J T, Bosse J L, He Q, Gao Y, Trassin M, Ye L, Clarkson J D, Wang C, Liu J, Salahuddin S, Ralph D C, Schlom D G, Iniguez J, Huey B D, Ramesh R 2014 Nature **516** 370
- <sup>101</sup>Zhao T, Scholl A, Zavaliche F, Lee K, Barry M, Doran A, Cruz M P, Chu Y H, Ederer C, Spaldin N A, Das R R, Kim D M, Baek S H, Eom C B, and Ramesh R 2006 Nat. Mater. **5** 823
- <sup>102</sup> Chu Y H, Martin L W, Holcomb M B, Gajek M, Han S J, He Q, Balke N, Yang C H, Lee D, Hu W, Zhan Q, Yang P L, Fraile-Rodríguez A, Scholl A, Wang S X, and Ramesh R 2008 Nat. Mater. **7** 478
- <sup>103</sup> Scheinfein M R, Unguris J, Kelley M H, Pierce D T, and Celotta R J 1990 Rev. Sci. Instrum. **61** 2501
- <sup>104</sup>Unguris J, Bowden S R, Pierce D T, Trassin M, Ramesh R, Cheong S W, Fackler S, and Takeuchi I 2014 Appl. Phys. Lett. Mater. **2** 076109
- <sup>105</sup>Qiu D Y, Ashraf K, and Salahuddin S 2013 Appl. Phys. Lett. **102** 112902
- <sup>106</sup>Zhou Z, Trassin M, Gao Y, Gao Y, Qiu D, Ashraf K, Nan T, Yang X, Bowden S R, Pierce D T, Stiles M D, Unguris J, Liu M, Howe B M, Brown G J, Salahuddin S, Ramesh R, and Sun N X 2015 Nat. Comm. **6** 6082
- <sup>107</sup>Wang J J, Hu J M, Peng R C, Gao Y, Shen Y, Chen L Q, and Nan C W 2015 Scientific Reports **5** 10459
- <sup>108</sup> Schlom D G, Chen L Q, Eom C B, Rabe K M, Streiffer S K, Triscone J M 2007 Annu. Rev. Mater. Res. **37** 589
- <sup>109</sup>Choi K J, Biegalski M, Li Y L, Sharan A, Schubert J, Uecker R, Reiche P, Chen Y B, Pan X Q, Gopalan V, Chen L Q, Schlom D G, and Eom C B 2004 Science **5** 1005
- <sup>110</sup>Devonshire A F 1954 Advances in Physics **3** 85

- 
- <sup>111</sup>Uwe H, and Sakudo T 1976 Phys. Rev. B **13** 271
- <sup>112</sup>Pertsev N A, Zembilgotov A G, and Tagantsev A K 1998 Phys. Rev. Lett. **80** 1988
- <sup>113</sup>Baek S H, Jang H W, Folkman C M, Li Y L, Winchester B, Zhang J X, He Q, Chu Y H, Nelson C T, Rzechowski M S, Pan X Q, Ramesh R, Chen L Q and Eom C B 2010 Nat. Mater. **9** 309
- <sup>114</sup>Xu R, Liu S, Grinberg I, Karthik J, Damodaran A R, Rappe A M, and Martin L W 2015 Nat. Mater. **14** 79
- <sup>115</sup>Chu Y H, Cruz M P, Yang C H, Martin L W, Yang P L, Zhang J X, Lee K, Yu P, Chen L Q, and Ramesh R 2007 Adv. Mater. **19** 2662
- <sup>116</sup>Nagarajan V, Ganpule C S, Li H, Salamanca-Riba L, Roytburd A L, Williams E D, and Ramesh R 2001 Appl. Phys. Lett. **79** 2805
- <sup>117</sup>Yu P, Luo W, Yi D, Zhang J X, Rossell M D, Yang C H, You L, Singh-Bhalla G, Yang S Y, He Q, Ramasse Q M, Erni R, Martin L W, Chu Y H, Pantelides S T, Pennycook S J, and R. Ramesh 2012 PNAS **109** 9710
- <sup>118</sup>Chu Y H, He Q, Yang C H, Yu P, Martin L W, Shafer P, and Ramesh R 2009 Nano Lett. **9** 1726
- <sup>119</sup>Chu Y H, Zhan Q, Martin L W, Cruz M P, Yang P L, Pabst G W, Zavaliche F, Yang S Y, Zhang J X, Chen L Q, Schlom D G, Lin I N, Wu T B, and Ramesh R 2006 Adv. Mater. **18** 2307
- <sup>120</sup>Feigl L, Yudin P, Stolichnov I, Sluka T, Shapovalov K, Mtebwa M, Sandu C S, Wei X K, Tagantsev A K, and Setter N 2014 Nat. Comm. **5** 4677
- <sup>121</sup>Jia C L, Urban K W, Alexe M, Hesse D, and Vrejoiu I 2011 Science **331** 1420
- <sup>122</sup>Tang Y L, Zhu Y L, Ma X L, Borisevich A Y, Morozovska A N, Eliseev E A, Wang W Y, Wang Y J, Xu Y B, Zhang Z D, Pennycook S J 2015 Science **348** 6234
- <sup>123</sup>Naumov I I, Bellaiche L, and Fu H 2004 Nature **432** 737
- <sup>124</sup>Kornev I, Fu H, and Bellaiche L 2004 Phys. Rev. Lett. **93** 196104
- <sup>125</sup>Aguado-Puente P, and Junquera J 2008 Phys. Rev. Lett. **100** 177601
- <sup>126</sup>Haeni J H, Irvin P, Chang W, Uecker R, Reiche P, Li Y L, Choudhury S, Tian W, Hawley M E, Craigo B, Tagantsev A K, Pan X Q, Streiffer S K, Chen L Q, Kirchoefer S W, Levy J, and Schlom D G 2004 Nature **430** 758
- <sup>127</sup>Vasudevarao A, Kumar A, Tian L, Haeni J H, Li Y L, Eklund C J, Jia Q X, Uecker R, Reiche P, Rabe K M, Chen L Q, Schlom D G, and Gopalan V 2006 Phys. Rev. Lett. **97** 257602
- <sup>128</sup>Fennie C J, and Rabe K M 2006 Phys. Re. Lett. **97** 267602
- <sup>129</sup>Lee J H, Fang L, Vlahos E, Ke X, Jung Y W, Kourkoutis L F, Kim J W, Ryan P J, Heeg T, Roeckerath M, Goian V, Bernhagen M, Uecker R, Hammel P C, Rabe K M, Kamba S, Schubert J, Freeland J W, Muller D A, Fennie C J, Schiffer P, Gopalan V, Johnston-Halperin E, and Schlom D G 2010 Nature **466** 954

- 
- <sup>130</sup>Becher C, Maurel L, Aschauer U, Lilienblum M, Magén C, Meier D, Langenberg E, Trassin M, Blasco J, Krug I P, Algarabel P A, Spaldin N A, Pardo J A, and Fiebig M 2015 *Nat. Nano.* **10** 661
- <sup>131</sup> Lee J H, and Rabe K M 2010 *Phys. Rev. Lett.* **104** 207204
- <sup>132</sup> Aschauer U, Pfenninger R, Selbach S M, Grande T, and Spaldin N A 2013 *Phys. Rev. B* **88** 054111
- <sup>133</sup> Fiebig M, Lottermoser Th, Fröhlich D, Goltsev A V, and Pisarev R V *Nature* **419** 818
- <sup>134</sup> Chanthbouala A, Garcia V, Cherifi R O, Bouzehouane K, Fusil S, Moya X, Xavier S, Yamada H, Deranlot C, Mathur N D, Bibes M, Barthélémy A, and Grollier J 2012 *Nat. Mater.* **11** 860
- <sup>135</sup> Gruverman A, Wu D, and Scott J F 2008 *Phys. Rev. Lett.* **100** 097601
- <sup>136</sup> Jo J Y, Yang S M, Kim T H, Lee H N, Yoon J G, Park S, Jo Y, Jung M H, and Noh T W 2009 *Phys. Rev. Lett.* **102** 045701
- <sup>137</sup> Chopdekar R V, Malik V K, Fraile Rodríguez A, Le Guyader L, Takamura Y, Scholl A, Stender D, Schneider C W, Bernhard C, Nolting F, and Heyderman L J 2012 *Phys. Rev. B* **86** 014408
- <sup>138</sup> Chopdekar R V, Heidler J, Piamonteze C, Takamura Y, Scholl A, Rusponi S, Brune H, Heyderman L J, and Nolting F 2013 *Eur. Phys. J. B* **86** 241
- <sup>139</sup> Denev S A, Lummen T T A, Barnes E, Kumar A, and Gopalan V 2011 *J. Am. Ceram. Soc.* **94** 2699
- <sup>140</sup> Kumar A, Denev S, Zeches R J, Vlahos E, Podraza N J, Melville A, Schlom D G, Ramesh R, and Gopalan V 2010 *Appl. Phys. Lett.* **97** 112903
- <sup>141</sup> Haislmaier R C, Podraza N J, Denev S, Melville A, Schlom D G, and Gopalan V 2013 *Appl. Phys. Lett.* **103** 031906
- <sup>142</sup> Lummen T T A, Gu Y, Wang J, Lei S, Xue F, Kumar A, Barnes A T, Barnes E, Denev S, Belianinov A, Holt M, Morozovska A N, Kalinin S V, Chen L Q, and Gopalan V 2014 *Nat. Comm.* **5** 3172
- <sup>143</sup> Trassin M, De Luca G, Manz S, and Fiebig M 2015 *Adv. Mater.* **27** 4871
- <sup>144</sup> Bibes M, and Barthélémy A 2008 *Nat. Mater.* **7** 425
- <sup>145</sup> Gajek M, Bibes M, Fusil S, Bouzehouane K, Fontcuberta J, Barthélémy A, and Fert A 2007 *Nat. Mater.* **6** 296
- <sup>146</sup> Scott J F 2007 *Nat. Mater.* **6** 256
- <sup>147</sup> Zhou Y 2011 *Nanotechnology* **22** 085202
- <sup>148</sup> Zhou Y, Woo C H, and Zheng Y 2012 *IEEE Trans. Nanotech.* **11** 77
- <sup>149</sup> Liu H, Bedau D, Backes D, Katine J A, Langer J, and Kent A D 2010 *Appl. Phys. Lett.* **97** 242510
- <sup>150</sup> Rowlands G E, Rahman T, Katine J A, Langer J, Lyle A, Zhao H, Alzate J G, Kovalev A A, Tserkovnyak Y, Zeng Z M, Jiang H W, Galatsis K, Huai Y M, Khalili Amiri P, Wang K L, Krivorotov I N, and Wang J P 2011 *Appl. Phys. Lett.* **98** 102509
- <sup>151</sup> Imre A, Csaba G, Ji L, Orlov A, Bernstein G H, Porod W 2006 *Science* **311** 205
- <sup>152</sup> Lambson B, Carlton D, and Bokor J 2011 *Phys. Rev. Lett.* **107** 010604

- 
- <sup>153</sup> Bhowmik D, You L, and Salahuddin S 2014 Nat. Nano. **9** 59
- <sup>154</sup> Roy K 2013 SPIN **3** 1330003
- <sup>155</sup> Roy K 2015 Sci. Rep. **5** 10822
- <sup>156</sup> Tour J M, and He T 2008 Nature **453** 42
- <sup>157</sup> Sawa A 2008 Mater. Today **11** 28
- <sup>158</sup> Yang J J, Strukov D B, and Stewart D R 2013 Nat. Nano. **8** 13
- <sup>159</sup> Wang X, Chen Y, Xi H, Li H, and Dimitrov D 2009 IEEE E. Dev. Lett. **30** 294
- <sup>160</sup> Khvalkovskiy A V, Zvezdin K A, Gorbunov Y V, Cros V, Grollier J, Fert A, and Zvezdin A K 2009 Phys. Rev. Lett. **102** 067206
- <sup>161</sup> Chanthbouala A, Matsumoto R, Grollier J, Cros V, Anane A, Fert A, Khvalkovskiy A V, Zvezdin K A, Nishimura K, Nagamine Y, Maehara H, Tsunekawa K, Fukushima A, and Yuasa S 2011 Nat. Phys. **7** 626
- <sup>162</sup> McGilly L J, Yudin P, Feigl L, Tagantsev A K, and Setter N 2015 Nat. Nano. **10** 145
- <sup>163</sup> Guo E J, Roth R, Herklotz A, Hesse A, and Dörr K 2015 Adv. Mater. **27** 1615
- <sup>164</sup> Van de Wiele B, Laurson L, Franke K J A, and van Dijken S 2014 Appl. Phys. Lett. **104** 012401
- <sup>165</sup> Whyte J R, and Gregg J M 2015 Nat. Comm. **6** 7361
- <sup>166</sup> Johann F, Morelli A, Vrejoiu I 2012 Phys. stat. sol. (b) **249** 2278
- <sup>167</sup> Roy K, Bandyopadhyay S, and Atulasimha J 2011 Phys. Rev. B **83** 224412
- <sup>168</sup> Hoffmann T, Thielen P, Becker P, Bohatý L, and M. Fiebig 2011 Phys. Rev. B **84** 184404
- <sup>169</sup> Garelo K, Avci C O, Miron I M, Baumgartner M, Ghosh A, Auffret S, Boule O, Gaudin G, and Gambardella P 2014 Appl. Phys. Lett. **105** 212402
- <sup>170</sup> Gu Z, Nowakowski M E, Carlton D B, Storz R, Im M Y, Hong J, Chao W, Lambson B, Bennett P, Alam M T, Marcus M A, Doran A, Young A, Scholl A, Fischer P, and Bokor J 2015 Nat. Comm. **6** 6466